

Density modulation and electrostatic self-consistency in a two-dimensional electron gas subject to a periodic quantizing magnetic field

Ulrich J. Gossmann, Andrei Manolescu* and Rolf R. Gerhardts

Max-Planck-Institut für Festkörperforschung, Heisenbergstrasse 1, D-70569 Stuttgart, Federal Republic of Germany

*Institutul de Fizica și Tehnologia Materialelor, C.P. MG-7 București-Măgurele, România

We calculate the single-particle states of a two-dimensional electron gas (2DEG) in a perpendicular quantizing magnetic field, which is periodic in one direction of the electron layer. We discuss the modulation of the electron density in this system and compare it with that of a 2DEG in a periodic electrostatic potential. We take account of the induced potential within the Hartree approximation, and calculate self-consistently the density fluctuations and effective energy bands. The electrostatic effects on the spectrum depend strongly on the temperature and on the ratio between the cyclotron radius R_c and the length scale $a_{\delta\rho}$ of the density variations. We find that $a_{\delta\rho}$ can be equal to the modulation period a , but also much smaller. For $R_c \sim a_{\delta\rho}$ the spectrum in the vicinity of the chemical potential remains essentially the same as in the noninteracting system, while for $R_c \ll a_{\delta\rho}$ it may be drastically changed by the Hartree potential: For noninteger filling factors the energy dispersion is reduced, like in the case of an electrostatic modulation, whereas for even-integer filling factors, on the contrary, the dispersion may be amplified.

I. INTRODUCTION

The interest in nonuniform magnetic fields, with spatial variations on a nanometer scale, has been stimulated by several recent experimental realizations, like magnetic quantum wells¹ or magnetic superlattices.²⁻⁵ In the quasi-classical regime of low magnetic fields, the theoretical investigations have concentrated on the commensurability oscillations of the resistivity,⁶⁻⁹ which are equivalent to the Weiss oscillations^{10,11} that occur in the presence of a periodic electrostatic potential.

The quantum regime of nonuniform magnetic fields with a strong variation of the order of 1 T within a distance of a few hundred nanometers is now experimentally accessible.¹² For this regime single-particle quantum mechanical calculations, concerning the tunneling through magnetic barriers or the bound states in magnetic wells, have recently been performed by Peeters, Matulis, and Vasilopoulos.^{13,14} Coulomb interaction effects have been discussed by Wu and Ulloa¹⁵ who studied the electron density distribution and the collective excitations in a magnetic superlattice with a short period, comparable to the average magnetic length. They found that the periodic magnetic field gives rise to an electron-density

modulation, which is reduced due to the counteracting induced electric field.

In the present paper we consider a two-dimensional electron gas (2DEG) in a perpendicular magnetic field of the form $B = B_0 + B_{mod}$ where B_0 is a homogeneous part and B_{mod} is, in the plane of the 2DEG, periodic in one direction with zero average. We describe in detail the charge-density response to the periodic part and the effects of the associated electrostatic potential. It will be very instructive to compare this situation with the modulation by a unidirectional periodic electrostatic potential $V_{ext}(x)$ (we include the charge $-e$ in the definition of the electrostatic potentials, which are therefore rather potential energies). The homogeneous part of the magnetic field is assumed to be strong enough so that a description in terms of Landau levels is adequate; we denote by $l_0 = \sqrt{\hbar/eB_0}$ and by $\omega_0 = eB_0/m$ the magnetic length and the cyclotron frequency associated with the uniform field B_0 . For a fixed mean electron density ρ_0 , the number of relevant Landau levels is of the order of the filling factor $\nu = (2\pi l_0^2)\rho_0$ and thus inversely proportional to the average magnetic field.

We first note that classically a magnetic field - modulated or not - has no influence in thermodynamic equilibrium because it drops out of the integral over momenta in the partition function (Bohr-van Leeuwen theorem¹⁶). Especially a magnetic modulation does not lead to a position dependence of the electron energy, which remains $mv^2/2$, and does not affect the equilibrium electron density. In contrast one expects (e. g. from Thomas-Fermi-theory) that modulation by an electrostatic potential should lead also to a modulation of the density $\delta\rho(x) = -(V_{ext}(x)/\mu)\rho_0$, where μ is the chemical potential. In the classical limit, i. e. for low average magnetic field with $\hbar\omega_0 \ll k_B T$, the density response of the 2DEG to electrostatic and to magnetic modulations is thus very different. A pure magnetic modulation does classically not give rise to electrostatic effects, whereas an external electrostatic potential is screened by the induced Hartree potential.

However, in the quantum regime of low filling factors the two types of modulation affect the density in a very similar manner: Both lift the degeneracy of the Landau levels and lead to dispersive bands. The homogeneous part B_0 of the magnetic field restricts the spatial extent of the relevant wavefunctions to the order of the cyclotron radius $R_c = l_0\sqrt{2n_F + 1}$ where n_F is the index of the Landau level at the chemical potential (that is n_F is the largest integer smaller than ν/g_s ; we assume

spin degeneracy $g_s = 2$ in this work). If n_F is small the modulation is typically slowly varying on the scale R_c and we can represent the Landau levels as functions $\epsilon_n(x)$, varying on the same length scale as the modulation. The width $\Delta\epsilon_n$ of these bands is of the order of $\hbar e\Delta B/m$ or ΔV , where ΔB and ΔV stand for the amplitude of the modulation of magnetic field and electrostatic potential, respectively. In this situation we expect that the density is determined by a “local” filling factor $\nu(x) = g_s \sum_n f(\epsilon_n(x))$, where $f(\epsilon)$ denotes the Fermi function. For temperatures satisfying $k_B T \ll \Delta\epsilon_n$, this must lead to a density modulation of order $(g_s/2\pi l_0^2)$ for both electric and magnetic modulations.

For an electric modulation it is known that, due to this strong effect of the Landau level dispersion on the density, the inclusion of the Coulomb interaction in the Hartree-approximation (which we will refer to as the electrostatically self-consistent system) changes drastically the spectrum of the system for low filling factors. Wulf *et. al.*¹⁷ found that, for filling factors not too close to an even-integer value, the self-consistent result corresponds to a nearly perfect screening of the modulating external potential and the Landau bands are flat within the order of $k_B T$. If for even-integer filling factor the chemical potential lies in a gap, the screening is much weaker although still considerable. For potentials strong enough to yield overlapping bands, $|\Delta\epsilon_n| > \hbar\omega_0$, the screening around even-integer filling factors becomes nonlinear, featuring two bands touching the Fermi level, and the width of the band n_F therefore locked to $\hbar\omega_0$.

The width of the Landau band at the Fermi level, however, is the basic element for understanding transport measurements^{6,3,18} and a major aim of this work is to investigate its behaviour for a magnetic modulation when electrostatic self-consistency is properly accounted for.

The paper is organized as follows. In section II we describe our model and the self-consistency problem in detail. In section III we treat the case of low filling factors, corresponding to a magnetic modulation varying slowly on the length scale R_c . In section IV we discuss the regime of lower average magnetic fields, where the cyclotron radius is not small against the period of the modulation. The numerical results we present are obtained using the material parameters of GaAs, namely the effective mass $m = 0.067m_e$ and the dielectric constant $\kappa = 12.4$. The average electron density is fixed to $\rho_0 = 2.4 \cdot 10^{11} \text{ cm}^{-2}$, chosen such that $\nu B_0 = 10 \text{ T}$, the period of the modulation is $a = 800 \text{ nm}$ and we consider values of B_0 between 10 T and 0.1 T corresponding to cyclotron radii between 7 nm and 740 nm.

II. DESCRIPTION OF THE MODEL

We consider an idealized 2DEG confined to the plane $\{\mathbf{r} = (x, y)\}$ and subject to a magnetic field $\mathbf{B}(\mathbf{r}) = (0, 0, B(x))$ which,^{7–9,15} within the plane, is directed in

z -direction, does not depend¹⁹ on y , and has a simple periodic dependence on x :

$$B(x) = B_0 + B_1 \cos Kx, \quad (1)$$

where $K = 2\pi/a$ is the wave vector of the modulation. We start with the noninteracting 2DEG described by the standard single-electron Hamiltonian $H^0 = (\mathbf{p} + e\mathbf{A})^2/2m$ in which we use the Landau gauge for the vector potential, $\mathbf{A}(x) = (0, B_0 x + (B_1/K) \sin Kx, 0)$. The eigenfunctions of H^0 depend on y only through a plane-wave prefactor,

$$\psi_{nX_0}(x, y) = L_y^{-1/2} e^{-iX_0 y/l_0^2} \phi_{nX_0}(x), \quad (2)$$

with L_y being a normalization length and X_0 the center coordinate. The functions $\phi_{nX_0}(x)$ are the eigenvectors of the one-dimensional Hamiltonian

$$H^0(X_0) = \hbar\omega_0 \left[-\frac{l_0^2}{2} \frac{d^2}{dx^2} + \frac{1}{2l_0^2} \left(x - X_0 + \frac{s}{K} \sin Kx \right)^2 \right], \quad (3)$$

where $s = B_1/B_0$ will be referred to as the modulation strength.

For the homogeneous system, $s = 0$, the functions $\phi_{nX_0}(x)$ are oscillator wave functions centered on X_0 , also known as Landau wave functions $\varphi_{nX_0}^L$, associated with the degenerate Landau levels $\epsilon_n^L = (n + 1/2)\hbar\omega_0$. The degeneracy is lifted for $s \neq 0$, and the resulting energy bands $\epsilon_n(X_0)$, together with the corresponding wave functions, can be obtained by diagonalizing the reduced Hamiltonian (3) in the basis of the Landau wave functions. The matrix elements can be written as

$$\begin{aligned} \langle \varphi_{nX_0}^L | H^0(X_0) | \varphi_{n'X_0}^L \rangle = \\ \hbar\omega_0 \left\{ \left(n + \frac{1}{2} \right) \delta_{nn'} + \frac{s}{2z} \left[E_{nn'}(z) + \sqrt{nn'} E_{n-1,n'-1}(z) \right. \right. \\ \left. \left. - \sqrt{(n+1)(n'+1)} E_{n+1,n'+1}(z) \right] \cos \left(KX_0 + (n-n')\frac{\pi}{2} \right) \right. \\ \left. + \frac{s^2}{8z} \left[\delta_{nn'} - E_{nn'}(4z) \cos \left(2KX_0 + (n-n')\frac{\pi}{2} \right) \right] \right\}, \quad (4) \end{aligned}$$

where $z = (Kl_0)^2/2$. We have used the notation:

$$\begin{aligned} E_{nn'}(z) &= \left(\frac{n'!}{n!} \right)^{1/2} e^{-z/2} z^{(n-n')/2} L_{n'}^{n-n'}(z) \\ &= (-1)^{n-n'} E_{n'n}(z), \quad (5) \end{aligned}$$

with $L_n^m(z)$ being a Laguerre polynomial. Applying first-order perturbation theory we get from (4) the energy levels as simple cosine-shaped bands

$$\epsilon_n^{PT1}(X_0) = \hbar\omega_0 \left[(n + 1/2) + s G_n(z) \cos(KX_0) \right] \quad (6)$$

where the factor $2s\hbar\omega_0 G_n(z) = s\hbar\omega_0 e^{-z/2} (2L_n^1(z) - L_n^0(z))$ has an oscillatory dependence on the ratio

$l_0\sqrt{2n+1}/a$ which is the basic reason for the commensurability oscillations seen in transport experiments.^{3,8} The limits of validity of Eq. (6) will be discussed below.

The single-particle density is given by the formula

$$\rho(x) = \frac{g_s}{2\pi l_0^2} \sum_{n=-\infty}^{\infty} \int_{-\infty}^{+\infty} dX_0 f(\epsilon_n(X_0)) |\phi_{nX_0}(x)|^2 \quad (7)$$

where $f(\epsilon)$ denotes the Fermi function and $g_s = 2$ accounts for spin degeneracy.

The density determines the electrostatic (Hartree) potential, which we treat by Fourier expansion $V^H(x) = \sum_{\eta \geq 1} V_\eta^H \cos(\eta Kx)$. Here

$$V_\eta^H = \frac{e^2}{4\pi\epsilon_0\kappa} \frac{a}{\eta} \rho_\eta = \frac{1}{\eta} \frac{a}{2\pi a_B} (2\pi l_0^2 \rho_\eta) \hbar\omega_0, \quad (8)$$

with $\rho(x) = \sum_{\eta \geq 0} \rho_\eta \cos(\eta Kx)$ and a_B the effective Bohr radius. For GaAs, $2\pi a_B \approx 63$ nm. We assume that the system is electrically neutral such that the average density ρ_0 does not contribute to V^H but only determines the chemical potential contained in the Fermi function. The Hartree potential has to be added to the Hamiltonian (3) and gives a contribution

$$\begin{aligned} & \langle \varphi_{nX_0}^L | V^H(x) | \varphi_{n'X_0}^L \rangle \\ &= \sum_{\eta} V_\eta^H E_{nn'}(\eta^2 z) \cos\left(\eta KX_0 + (n - n')\frac{\pi}{2}\right) \end{aligned} \quad (9)$$

to the matrices (4). The strongest influence on the induced potential originates from the low Fourier components of the density, which are related to the long-range charge fluctuations. We diagonalize the Hamiltonian $H^0(X_0) + V^H$ self-consistently with Eq. (7) by a numerical iterative scheme.

To understand the way the system achieves self-consistency, we occasionally consider also a 2DEG subject to a homogeneous magnetic field B_0 and a cosine electrostatic potential

$$V_1(x) = V_1 \cos(Kx) \quad (10)$$

with modulation strength $v_1 = V_1/\hbar\omega_0$ instead of the magnetically modulated system (1). First-order perturbation theory yields for the electric modulation (10) the spectrum

$$\epsilon_n^{PT1}(X_0) = \hbar\omega_0 \left[(n + 1/2) + v_1 F_n(z) \cos(KX_0) \right] \quad (11)$$

with $F_n(z) = e^{-z/2} L_n(z)$.

III. THE LIMIT OF LONG PERIOD

In this section we deal with a long-period magnetic modulation, with a strong average magnetic field, such

that $Kl_0 \ll 1$ and $R_c \sim l_0$ (but not necessarily with $B_1 \ll B_0$). Approximate analytical results for both electric and magnetic modulations will be developed for a better understanding of the energy spectra and electron density. We first describe the properties of the noninteracting system.

A. Noninteracting electrons

Treating the magnetic modulation as a perturbation presents some difficulties in this limit, since for nonvanishing s and $z \rightarrow 0$ the matrix elements $\langle \varphi_{nX_0}^L | H^0(X_0) | \varphi_{n+mX_0}^L \rangle$ given by Eq. (4) diverge for $m = 0, \pm 1$, while those with $m = \pm 2$ are finite and those with $|m| > 2$ vanish. Thus the Hamiltonian matrix becomes band-diagonal, and the divergent elements cancel in a complicated way in order to yield finite eigenvalues. Therefore, for $Kl_0 \ll 1$ an accurate numerical diagonalization requires a large matrix (4) and the Landau level mixing is strong, except if $s \rightarrow 0$. This complication does not occur for the electric modulation (10) for which the Landau wave functions diagonalize the matrix in the long-period limit for any v_1 , and first-order perturbation theory gives the *exact* energy spectrum for $z \rightarrow 0$, namely¹⁸ $\epsilon_{nX_0} = (n + 1/2)\hbar\omega_0 + V \cos(KX_0)$.

Instead of using standard perturbation theory with respect to the modulation strength s , we can handle the Hamiltonian (3) by performing a Taylor expansion of the potential term $(\hbar\omega_0/2l_0^2)(x - X_0 + \frac{s}{K} \sin Kx)^2$ around its minimum X_1 given by

$$X_1 = X_0 - \frac{s}{K} \sin KX_1. \quad (12)$$

For fixed KX_0 and $|s| < 1$ this has a unique solution KX_1 with $X_1 = X_0$ for $KX_0 = 0, \pi$. The parabolic approximation reads

$$H^0(X_0) \approx \hbar\omega_0 \left[-\frac{l_0^2}{2} \frac{d^2}{dx^2} + \frac{(1 + s \cos KX_1)^2}{2l_0^2} (x - X_1)^2 \right], \quad (13)$$

with an error term of order $s \hbar\omega_0 Kl_0 ((x - X_1)/l_0)^3$ from which we can show that (13) yields the eigenvalues and the density for low filling factors correct to leading order in Kl_0 . The Hamiltonian (13) is equivalent to the unperturbed one, Eq.(3), but with modified center coordinate X_1 , cyclotron frequency $\tilde{\omega}_0 = \omega_0(1 + s \cos(KX_1))$ and magnetic length $\tilde{l}_0 = l_0/\sqrt{1 + s \cos(KX_1)}$. The main effect of the magnetic modulation on the wave functions is the shift (12) of their center of weight. We see that, since $K(X_1 - X_0)$ is independent of K , the absolute shift $X_1 - X_0$ increases with increasing modulation period ($K \rightarrow 0$) at equivalent positions within the period (i. e. for fixed KX_0) except for $KX_0 = 0, \pi$. This explains the difficulties with the standard perturbation

theory which expands the shifted Landau functions with center $X_1(X_0)$ in the basis of Landau functions centered around X_0 .

The Landau bands resulting from Eq.(13) are

$$\epsilon_n(X_0) = \hbar\omega_0 \left(1 + s \cos(KX_1(X_0))\right) \left(n + \frac{1}{2}\right). \quad (14)$$

The appearance of X_1 instead of X_0 in Eq. (14) leads to a substantial deviation of the simple cosine band shape predicted by first-order perturbation theory; the bandwidth is, however, given correctly by Eq. (6). In calculating the density, the indicated replacement of l_0 by \tilde{l}_0 leads to corrections of higher order in Kl_0 and, since this order is not included correctly, is not to be used. We therefore insert just shifted Landau-functions into Eq. (7) and obtain

$$\begin{aligned} \rho(x) &= \frac{g_s}{2\pi l_0^2} \sum_n \int dX_0 f(\epsilon_n(X_0)) |\varphi_{n,X_1(X_0)}^L(x)|^2 \\ &= \frac{g_s}{2\pi l_0^2} \sum_n \int dX_1 \frac{dX_0}{dX_1} f(\epsilon_n(X_0(X_1))) |\varphi_{n,X_1}^L(x)|^2. \end{aligned} \quad (15)$$

From (12) we have $dX_0/dX_1 = 1 + s \cos(KX_1)$ and with (14) for the energy spectrum we finally get

$$\begin{aligned} \rho(x) &= \frac{g_s}{2\pi l_0^2} \sum_n \int dX_1 \left(1 + s \cos(KX_1)\right) \\ &\times f\left(\hbar\omega_0 [1 + s \cos(KX_1)] (n + 1/2)\right) |\varphi_{n,X_1}^L(x)|^2. \end{aligned} \quad (16)$$

Both results (14) and (16) turn out to be reliable within a relative accuracy of $(s K R_c)$. They can also be derived by a simple variational approach, using a set of translated oscillator states $\varphi_{n,X_0+u}^L(x)$ as trial wave functions and taking the limit $z \rightarrow 0$ after minimizing the expectation value of the energy.²⁰ The numerical results which we shall present are obtained from a diagonalization of (4), however.

We note that for the electric modulation (10) the results corresponding to Eqs. (12), (14) and (16) read $X_1 = X_0 + v_1 Kl_0^2 \sin KX_1$,

$$\begin{aligned} \epsilon_n(X_0) &= \hbar\omega_0 \left[n + 1/2\right. \\ &\left.+ v_1 \left(1 - (1/2)(n + 1/2)(Kl_0)^2\right) \cos(KX_1)\right] \end{aligned} \quad (17)$$

and

$$\begin{aligned} \rho(x) &= \frac{g_s}{2\pi l_0^2} \sum_n \int dX_1 \left(1 - v_1 (Kl_0)^2 \cos(KX_1)\right) \\ &\times f\left(\hbar\omega_0 [n + 1/2 + v_1 \cos(KX_1)]\right) |\varphi_{n,X_1}^L(x)|^2. \end{aligned} \quad (18)$$

The error term in the Taylor expansion around X_1 is here of order $v_1 \hbar\omega_0 (Kl_0)^3 ((x - X_1)/l_0)^3$ and permits inclusion of the $(Kl_0)^2$ terms. The total width of the bands from

(17) is also obtained from the result (11) of perturbation theory by expansion around $Kl_0 = 0$ up to order $(Kl_0)^2$.

We see from Eqs. (17,18) that for a long-period cosine *electric* modulation the bands follow the potential with constant width and the states are not changed by the modulation; consequently the density is only affected by the dispersion of the levels via the argument of the Fermi function. In contrast, for a *magnetic* modulation according to (14) the widths of the Landau bands increase linearly with n and the X_1 -dependent prefactor of the Fermi function in (16) does not decrease with increasing period.

In Fig. 1 the dashed lines show the modulation of the density of the noninteracting system with a magnetic modulation of amplitude $B_1 = 0.1$ T for different values of the filling factor between 4 and 6 obtained by sweeping B_0 ; the temperature is 1 K, so that $k_B T$ is much smaller than $s\hbar\omega_0$. The density is given in units of $1/(2\pi l_0^2)$ so that the mean value of each line equals ν . The lines for the even-integer values of the filling factor, $\nu = 4, 6$, are marked with circles. They show a cosine form, where the amplitude is larger for $\nu = 6$ than for $\nu = 4$. This behaviour is easily derived from Eq. (16); since here the chemical potential lies in a gap, the Fermi function is either 0 or 1, and the integral gives to leading order in Kl_0

$$\delta\rho(x) |_{\nu \text{ small and even}} = (s\nu/2\pi l_0^2) \cos Kx. \quad (19)$$

In the corresponding result for the electric modulation, the factor s is replaced by $-v_1(Kl_0)^2$ which has a different sign and vanishes for $Kl_0 \rightarrow 0$. The persistence of a finite density modulation at even-integer filling factors for a period much longer than the magnetic length constitutes a major difference between the two types of modulation for strong average magnetic fields. Note that the result (19) can also be written in the form $\rho(x) = \nu/2\pi l^2(x)$ (ν small and even) where $l(x) = \sqrt{\hbar/eB(x)}$ is the magnetic length corresponding to the local field $B(x)$. This means that we can in the long-period limit think of the magnetic modulation as changing the local degeneracy of the Landau levels, thus leading to a modulated density even for spatially constant filling factor (in this work we use the notion of an x -dependent filling factor $\nu(x)$ as just counting the number of locally occupied bands, which makes sense of course only in the long-period limit).

The dashed lines between the ones with circles in Fig. 1 show the behaviour of the density while the $n = 2$ level is successively filled. Due to the energy dispersion (14) and the low temperature, the $n = 2$ states around $KX_0 = \pi$ are occupied first, forming a region with local filling factor $\nu(x) = 6$ while around $KX_0 = 0, 2\pi$ we still have $\nu(x) = 4$ until the total filling closely approaches 6. Since the spatial extent of the wavefunctions is small compared to the period a , the difference in density between these two regions is of order $g_s/(2\pi l_0^2)$. We observe, however, that within a region of constant local filling factor the density is not constant but follows the cosine shape imposed by Eq.(19) with ν replaced by the appropriate local filling factor $\nu(x)$.

B. Self-Consistent System

Since the density profiles of the noninteracting system correspond, according to Eq. (8), to electrostatic potentials with amplitudes larger than $\hbar\omega_0$, we expect substantial changes in the spectrum when we take electrostatic self-consistency properly into account, as we do now. The resulting densities are plotted as solid lines in Fig. 1 and show much smaller fluctuations. In Fig. 2 we show results for a magnetic modulation of $B_1 = 0.1$ T at filling factors (a) $\nu = 5$, (b) $\nu = 4$ and (c) $\nu = 14.3$ corresponding to average fields $B_0 = 2.0$ T, 2.5 T and 0.7 T, respectively. The upper panel displays the self-consistent spectra for temperatures $T = 1$ K and $T = 0.1$ K together with the noninteracting spectra, the lower panel shows the corresponding self-consistent densities. More data for the self-consistent bandwidths and the density amplitudes in this regime are also displayed in Fig. 5 and 6 which are discussed in section IV B.

When the total filling factor is small and not too close to an even-integer value, the regions of increased density correspond to the minima of the Landau bands (cf. Fig. 1). Therefore the generated Hartree potential, which is maximum at maximum electron density, will act to *reduce* the dispersion of the not fully occupied band with index n_F . The self-consistent solution yields then a very flat (“pinned”) band with deviations of only the order of $k_B T$ from the chemical potential, and the local filling factor is fractional over the whole period. This situation is shown in Fig. 2 (a) for an odd-integer average filling factor $\nu = 5$. The self-consistent potential here has to cancel the dispersion of the not fully occupied level n_F , which is larger than the dispersion of the levels with $n < n_F$. Thus the potential is $V^H(x) \approx -s \hbar\omega_0 (n_F + 1/2) \cos Kx$ and the dispersion of the levels with $n < n_F$ is reversed in sign.

For even-integer filling factor, however, according to Eq. (19) the regions of increased density correspond to maxima of the Landau bands, since both $\rho(x)$ and $\epsilon_n(X_0)$ follow the shape of the magnetic modulation with positive sign. Consequently, the potential generated by the density modulation (19) *increases* the dispersion of the highest occupied band n_F instead of acting against the modulation broadening. If the magnetic modulation is sufficiently weak, the resulting self-consistent potential can be calculated by combining Eqs. (16), (18) and (8) as $V^H(x) = \tilde{V}_H \cos Kx$ (ν small and even) where

$$\tilde{V}_H = \frac{sw\hbar\omega_0\nu}{1 + w(Kl_0)^2\nu} \quad (20)$$

and $w = a/2\pi a_B \gg 1$. This linear behaviour breaks down, however, if the resulting bandwidth $|\Delta\epsilon_{n_F}| = 2s\hbar\omega_0(n_F + 1/2) + 2\tilde{V}_H$ exceeds $\hbar\omega_0$. In this case the next-higher band reaches the chemical potential around $KX_0 = \pi$ and the self-consistent solution (shown in Fig. 2 (b) for $\nu = 4$) features a region around $KX_0 = 0, 2\pi$ where the band n_F is pinned to μ , a region around

$KX_0 = \pi$ where the band $n_F + 1$ is pinned to μ and a region in between where the chemical potential lies in a gap and the density still follows the cosine shape (19). As described in section I, similar effects of electrostatic self-consistency are obtained for an electrically modulated system,¹⁷ but there the bandwidth of the highest occupied band is always reduced compared to the non-interacting results. Then, a modulation strength $v_1 > 1$ is needed to produce the formation of pinned regions at even-integer filling factors, whereas in the magnetic case only $sw \sim 1$ must be satisfied.

For the parameters of Fig. 2 (c) the bands of the non-interacting system do overlap at the Fermi level due to the linear increase of their width with n . In this situation the density fluctuations and the induced potentials consist mainly of higher Fourier components. The corresponding wavelengths $2\pi/\eta K$, with $\eta > 1$, are comparable to R_c , even though $R_c \ll a$ is still satisfied. We therefore cannot discuss the effects of the Hartree potential here within the limit of a long period but instead we have to consider the density response for electric modulations with $a \sim R_c$. This is done in the next section. We observe, however, that in Fig. 2 (c) the spectrum around the Fermi level remains essentially unchanged although we can tell from the behaviour of the lowest level that a considerable electrostatic potential does exist.

For the lower temperature $T = 0.1$ K the density traces in Fig. 2 (b) and very pronounced in (c) show also superimposed short-period oscillations. These have their origin in the nodes and maxima of the wavefunctions and can also be reproduced by Eq. (16) with the Landau functions $\varphi_n^L(x)$.

IV. R_c COMPARABLE WITH PERIOD

In this section we discuss properties of the modulated system obtained when for fixed modulation amplitude B_1 the average field B_0 is lowered so that we enter the regime where R_c is no longer small compared to the period a . In this case the approximation of the modulation by the first terms of a Taylor series breaks down and its actual functional form becomes important. However, the numerical method outlined in section II is still valid provided that $s < 1$, i. e. the total magnetic field $B(x)$ is nowhere vanishing. We consider first the noninteracting system.

A. Noninteracting Electrons

The quantity we are most interested in is the amplitude $\Delta\epsilon_{n_F}$ of the Landau level n_F at the Fermi energy. In Fig. 3 (a) (solid line) this bandwidth is shown for a weak magnetic modulation $B_1 = 0.01$ T and average fields B_0 in the range 10 T $> B_0 > 0.125$ T. Starting from high fields at $B_0 = 10$ T we have first $n_F = 0$

and the bandwidth is $s\hbar\omega_0$. When the field is lowered, $|\Delta\epsilon_{n_F}|$ increases in steps of $2s\hbar\omega_0$ at even-integer filling factors, that is when n_F jumps by one, as follows from (14). When $2R_c/a$ becomes larger than about $1/4$ the increase of $|\Delta\epsilon_{n_F}|$ becomes visibly slower and goes over into an oscillatory behaviour with the first maximum at about $2R_c = 0.6a$. This can be understood with the result (6) of first-order perturbation theory. Using the asymptotic relation between Laguerre polynomials and Bessel functions we obtain for the bandwidth at the Fermi level from (6) the formula⁹

$$|\Delta\epsilon_{n_F}| \approx \left| 2s\hbar\omega_0 A_m J_1(KR_c) \right| \quad (21)$$

where J_1 is the Bessel function of order 1, $R_c = l_0\sqrt{2n_F + 1}$, and $A_m = (R_c/Kl_0^2)$. The expression (21) describes well the bandwidths (also for small filling factors) as long as the average field is strong enough to ensure $s \ll 1$. It has zeros at approximately

$$KR_c = (\lambda + 1/4)\pi, \lambda = 1, 2, \dots \quad (22)$$

corresponding to a flat-band with vanishing dispersion at the Fermi level.⁶ For our parameters we encounter only the first ($\lambda = 1$) of these magnetic flat-band situations around $B_0^{-1} = 6.2 \text{ T}^{-1}$. From Eq.(21) we infer further that the maximum values of the bandwidth at the Fermi level are of order $2s\hbar\omega_0 A_m$ rather than $2s\hbar\omega_0$. If we replace in R_c the discrete $2n_F + 1$ by ν , the factor A_m becomes $\sqrt{a^2\rho_0/\pi g_s}$ and depends thus only on the period and mean density; typically we have $A_m > 10$, e. g. for our parameters $A_m = 15.6$. Consequently a seemingly weak modulation strength $s \sim (1/A_m) \ll 1$ is sufficient to yield for KR_c around a maximum of the Bessel function J_1 a bandwidth $|\Delta\epsilon_{n_F}| > \hbar\omega_0$ which means that the bands around the Fermi level do overlap. In Fig. 4 (a) the bandwidth at the Fermi level for a modulation of $B_1 = 0.1 \text{ T}$ is plotted; it is larger than $\hbar\omega_0$ for $B_0 < 1 \text{ T}$. For this stronger modulation the spectra show, at fields $B_0 < 0.25 \text{ T}$, also substantial deviations from the first-order perturbation expression (6), because the modulation strength s then becomes too large. The bands around the Fermi level are not cosine-shaped in this regime but have extrema away from $KX_0 = 0, \pi$. As a consequence, the bandwidth does not go through a zero at the flat-band condition (22) although its behaviour still resembles the oscillations described by (21).

For an electric modulation the result corresponding to (21) is $|\Delta\epsilon_{n_F}| = \left| 2v_1\hbar\omega_0 J_0(KR_c) \right|$ with zeros at $KR_c = (\lambda - 1/4)\pi, \lambda = 1, 2, \dots$ (these are the electric flat-band situations) and the bandwidth is always smaller than $2v_1\hbar\omega_0$. In Fig.(3) (a) the bandwidth at the Fermi level for an electric modulation of amplitude $V_1 = 0.27 \text{ meV} = A_m(\hbar e/m) \cdot 0.01 \text{ T}$ is shown as dashed line; the modulation amplitude is chosen such that the bandwidths are comparable to the ones induced by the magnetic modulation also depicted in this figure.

In describing the induced density fluctuations $\delta\rho(x) = \rho(x) - \rho_0$ we face the difficulty that these have in general no simple shape (see Fig. 1). As a measure of their magnitude we therefore concentrate on their amplitude $|\Delta\rho|$. This quantity is displayed in units of $(1/2\pi l_0^2)$ for the non-interacting case at temperatures $T = 1 \text{ K}$ and $T = 0.1 \text{ K}$ in Fig. 3 (b) for a weak magnetic modulation not leading to band overlap and in Fig. 4 (b) for a stronger modulation with overlapping bands. The lower temperature $T = 0.1 \text{ K}$ corresponds to $k_B T = 8.6 \cdot 10^{-3} \text{ meV}$ which in the displayed range of B_0 can be considered as small compared to $\hbar\omega_0$ whereas for the higher temperature $T = 1 \text{ K}$ the finite size of $k_B T$ becomes important for about $B_0^{-1} > 3 \text{ T}^{-1}$. The results for the density can be summarized as follows: If the bands around the Fermi level do not overlap and $k_B T$ is small against $\hbar\omega_0$ and also against the gap between the bands n_F and $n_F + 1$, then for even-integer filling factor the density is cosine-shaped $\delta\rho(x)|_{\nu \text{ even}} = sr_m(KR_c) \cos(Kx)$. This is due to the distortion of the occupied wavefunctions by the modulated magnetic field. The amplitude r_m is for $KR_c \rightarrow 0$ equal to the total density ρ_0 (see Eq. (19)) and shows for lower fields oscillations in KR_c with zeros at both electric and magnetic flat-band situations. During the filling of each band, i. e. when the filling factor is not an even integer, an additional density fluctuation of the order of $(1/2\pi l_0^2)$ is produced due to the dispersion of the bands, like in Fig. 1. Both effects have a tendency to cancel each other. If $k_B T$ is not small compared to $\hbar\omega_0$ or to the gap between the bands n_F and $n_F + 1$, this cancellation becomes almost perfect and the resulting density modulation is minute. If the bands around the Fermi level do overlap (as in Fig. 4 (b) for $B_0 < 1 \text{ T}$), the density has a complicated shape with several extrema and its amplitude shows an irregular dependence on the filling factor. For $k_B T \ll \hbar\omega_0$ the amplitude of the density fluctuations is still of the order of $1/2\pi l_0^2$ (but not larger) whereas for a higher temperature again no appreciable modulation of the density is produced.

We see thus that the modulated magnetic field affects the density only if R_c is small compared to the modulation period or if the temperature is very low; in any case the resulting density modulation is limited in amplitude by $g_s/2\pi l_0^2$. For not too low temperatures the Thomas-Fermi-prediction, namely no modulation of the density, holds to good accuracy as soon as $R_c > a/4$.

The density amplitudes resulting from an electric modulation are shown in Fig. 3 (c). As discussed in section III A, we find for $R_c < a/8$ density fluctuations of order $g_s/2\pi l_0^2$ if the level n_F is partially occupied, and essentially no modulation of the density at even-integer filling factors. For lower fields B_0 , however, the density modulation becomes dominated by a cosine contribution whose amplitude is not related to $g_s/2\pi l_0^2$ but rather equals the Thomas-Fermi value

$$\delta\rho_{\text{TF}}(x) = -(V(x)/\mu)\rho_0 \quad . \quad (23)$$

Since $\delta\rho_{\text{TF}}$ is independent of B_0 it appears in the plotted

quantity $2\pi l_0^2 |\Delta\rho|$ as a linearly increasing background. For the higher temperature we find that for $R_c > a/4$ the density is described accurately by Eq. (23), i. e. $\delta\rho(x) = -(v_1 \hbar \omega_0 / \mu) \rho_0 \cos(Kx)$. For the lower temperature deviations from this result appear which are of similar magnitude as the corresponding deviations from zero for the magnetic modulation (except that at even-integer filling factors they do not vanish at the magnetic flat-band condition but only at the electric one). The density modulation for the low temperature and even-integer filling factor is entirely due to the distortion of the occupied wavefunctions and follows very well the formula derived by Aleiner and Glazman²¹ from first-order perturbation theory. Most important for our purposes is the fact that in any case for $R_c > a/4$ there exists an appreciable modulation of the density, whose main part is a wave-function effect and follows the electrostatic potential linearly, independent of the spectrum at the Fermi level. Due to the linearity in V , it is clear that this applies also to the density response to those higher Fourier components of a non-cosine electrostatic potential whose wavevectors ηK satisfy $\eta K R_c > 1$.

B. Self-Consistent System

Having discussed the density response induced by modulated magnetic and electric fields, we now proceed with the investigation of the effects of electrostatic self-consistency for the magnetically modulated system. In Fig. 5 and 6 (a) and (b) the bandwidth at the Fermi level of the self-consistent system and the amplitude of the Hartree potential $|\Delta V^H|$ are shown for the same parameters as used in Fig. 3 and 4, respectively. The bandwidth of the noninteracting system and $\hbar\omega_0$ are also shown for comparison. We can clearly distinguish the high-field regime (limited by $R_c < a/4$) discussed in section III where the spectrum around the Fermi level is dominated by the electrostatic effects: Instead of the monotonous increase in the noninteracting system the bandwidth at the Fermi level is here of order $k_B T$ when the filling factor is not close to an even-integer value and has at even-integer filling factors sharp maxima with a height of the order $\hbar\omega_0$ (this value is reached only for the stronger modulation in Fig. 6 while in Fig. 5 Eq. (20) remains valid). The amplitude of the potential equals the difference of the self-consistent and noninteracting bandwidths, reflecting the fact that electrostatic self-consistency is achieved by adjusting the spectrum.

For lower fields with $R_c > a/4$ the electrostatic corrections to the bandwidth at the Fermi level become much less pronounced and the validity of (21) is eventually restored well before the first magnetic flat-band situation. The main reason for this is that now the Hartree potential is able to affect the density independently of the dispersion at the Fermi level. Consequently, self-consistency can be achieved without changing $|\Delta\epsilon_{n_F}|$.

We first discuss the weaker modulation without band overlaps (Fig. 5). Here, for the higher temperature, the density modulation produced by the periodic magnetic field is already small without inclusion of the Hartree potential so that the self-consistent potential is also minute. But also for the lower temperature in (b) the situation changes around $R_c = a/4$ and the bandwidths become close to the noninteracting values, although the amplitude of the self-consistent potential remains appreciable. Around $R_c = (3/8)a$ an electric flat-band condition is satisfied and the first Fourier component of the Hartree-potential has no effect on $|\Delta\epsilon_{n_F}|$. Therefore here the change of the bandwidth at the Fermi level due to the Hartree-potential must be small but this is not reflected in the amplitudes of the self-consistent densities and potentials. For still lower fields, away from the electric flat-band situation, the Hartree potential yields again noticeable corrections to the bandwidths but the noninteracting curve remains essentially valid.

For the stronger modulation displayed in Fig. (6), the noninteracting bandwidth at the Fermi level is recovered as soon as it gets larger than $\hbar\omega_0$. Since the bands at the Fermi level then overlap, the density modulation consists mainly of higher Fourier components with wave vectors ηK , $\eta > 1$. The induced potential therefore belongs already to the regime of validity of the linear relation (23) although we still have $R_c < a/8$. Therefore the Hartree potential here reduces the density modulation in amplitude but does not much alter its shape, while the bands around the Fermi level remain dominated by the cosine form imposed by the periodic magnetic field.

V. CONCLUSION

We have calculated the density response of a 2DEG in a quantizing magnetic field B_0 to a magnetic cosine modulation $B_1 \cos(Kx)$ and compared it with the response to an electric cosine modulation. We also included self-consistently the induced electrostatic potentials which reduce the density fluctuations. We investigated in detail the changes in the energy spectrum brought about by the requirement of electrostatic self-consistency. In contrast to the case of an electric modulation, where the Hartree potential always tends to decrease the width of the Landau bands, for a magnetic modulation the Hartree potential may either decrease or increase the band dispersion, depending on strength and period of the modulation and on the filling factor.

In any case the produced density modulation depends crucially on the temperature. If $k_B T$ is not small compared to $\hbar\omega_0$ the behaviour of the density is quasi-classical, i. e. the periodic magnetic field does not lead to an appreciable density modulation, while the density modulation induced by an electrostatic potential essentially follows the Thomas-Fermi formula. For temperatures satisfying $k_B T \ll \hbar\omega_0$ (which we assume in the

remainder of this section) both types of modulation lead to an appreciable non-classical inhomogeneity of the density and thus to a non-trivial electrostatic self-consistency problem.

We were mainly interested in the effect of the Hartree-potential on the spectrum around the chemical potential. We found that an important parameter is the ratio of the cyclotron radius to the length scale a_{ϕ} of the density variation. If the bands in the vicinity of the Fermi level do not overlap we have $a_{\phi} \sim a$, whereas for overlapping bands the density fluctuations consists of higher Fourier components and a_{ϕ} is significantly smaller than the period a of the modulation. Concerning electrostatic effects we can clearly distinguish two regimes by the conditions $R_c \ll a_{\phi}/4$ and $R_c \gtrsim a_{\phi}/4$. This defines for fixed total density a distinction between high and lower average magnetic fields. The value of B_0 around which the regime changes depends for a weak modulation only on the period while for a sufficiently strong modulation the transition takes place when the bands start to overlap.

For a_{ϕ} much larger than the cyclotron radius, i. e. for high enough B_0 , the dispersion of the energy levels is changed drastically by the inclusion of electrostatic self-consistency. As in the case of a purely electrostatic modulation, for which similar screening effects are known,¹⁷ the effective Landau bands may be pinned to the Fermi level over regions comparable to the period. The nonuniform magnetic field affects the density also in regions where the chemical potential lies in a gap between two bands. In those regions the density is not constant but reproduces the profile of the magnetic field, since the latter alters the number of states in the vicinity of each center coordinate.

If the cyclotron radius is not small enough against a_{ϕ} , $R_c \gtrsim a_{\phi}/4$, the inclusion of electrostatic self-consistency does not lead to an appreciable change of the dispersion of the bands around the Fermi level. The behaviour of the latter in the regime where $R_c \sim a$ can therefore safely be calculated from the noninteracting system.

VI. ACKNOWLEDGEMENTS

We thank Daniela Pfannkuche for fruitful discussions. One of us (A. M.) is grateful to the Max-Planck-Institut für Festkörperforschung, Stuttgart, for hospitality and support. This work was supported by the German Bundesministerium für Bildung und Forschung (BMBF).

- ⁴ S. Izawa, S. Katsumoto, A. Endo, and Y. Iye, J. Phys. Soc. Japan **64**, 706 (1995)
- ⁵ P. D. Ye, *et al.*, Appl. Phys. Lett. **67**, 1441 (1995).
- ⁶ P. Vasilopoulos and F. M. Peeters, Superlatt. Microstruct. **7**, 393 (1990).
- ⁷ D. P. Xue and G. Xiao, Phys. Rev. B **45**, 5986 (1992).
- ⁸ F. M. Peeters and P. Vasilopoulos, Phys. Rev. B **47**, 1466 (1993).
- ⁹ R. R. Gerhardts, Phys. Rev. B **53**, 11 064 (1996).
- ¹⁰ D. Weiss, K. v. Klitzing, K. Ploog, and G. Weimann in Proc. of Int. Conf. Application of High Magnetic Fields in Semi-conductor Physics, Würzburg, 1988, G. Landwehr, ed., Vol. 87 of Springer Series in Solid State Sciences, Springer Verlag 1989; Europhys. Lett. **8**, 179 (1989)
- ¹¹ R. R. Gerhardts, D. Weiss, and K. v. Klitzing, Phys. Rev. Lett. **62**, 1173 (1989); R. W. Winkler, J. P. Kotthaus, K. Ploog *ibid.* **62**, 1177 (1989).
- ¹² D. Weiss and P. D. Ye, private communication.
- ¹³ F. M. Peeters and A. Matulis, Phys. Rev. B **48**, 15 166 (1993).
- ¹⁴ A. Matulis, F. M. Peeters, and P. Vasilopoulos, Phys. Rev. Lett. **72**, 1518 (1994).
- ¹⁵ X. Wu and S. E. Ulloa, Phys. Rev. B **47**, 7182 (1993).
- ¹⁶ see e. g. J. H. van Vleck, *The theory of Electric and Magnetic Susceptibilities*, Oxford University Press, London, 1932.
- ¹⁷ U. Wulf, V. Gudmundsson, and R. R. Gerhardts, Phys. Rev. B **38**, 4218 (1988).
- ¹⁸ C. Zhang and R. R. Gerhardts, Phys. Rev. B **41**, 12 850 (1990).
- ¹⁹ Energy spectra for a 2D magnetic superlattice were calculated by R. R. Gerhardts, D. Pfannkuche, and V. Gudmundsson, Phys. Rev. B **53**, 9591 (1996).
- ²⁰ A. Manolescu, Phys. Rev. B **45**, 11 829 (1992).
- ²¹ I.L. Aleiner and L.I. Glazman Phys. Rev. B **52**, 11296 (1995).

FIG. 1. Density $\rho(x)$ in units of $1/2\pi l_0^2$ for a magnetic modulation of amplitude $B_1 = 0.1$ T in average fields $B_0 = 2.5 - 1.7$ T corresponding to filling factors $\nu = 4 - 6$. The temperature is $T = 1$ K. The dashed lines are for the noninteracting system; the results for $\nu = 4$ and $\nu = 6$ are marked with circles. The lines between these two show the successive filling of the $n = 2$ level when ν is increased in steps of $1/3$. The solid lines display the results for the same filling factors after establishing electrostatic self-consistency.

FIG. 2. Results for a magnetic modulation of amplitude $B_1 = 0.1$ T at (a) $\nu = 5$ ($B_0 = 2.0$ T), (b) $\nu = 4$ ($B_0 = 2.5$ T) and (c) $\nu = 14.3$ ($B_0 = 0.7$ T). The upper panel displays the spectra (dashed lines: noninteracting, solid lines: self-consistent solution at $T = 1$ K, dash-dotted lines: self-consistent solution at $T = 0.1$ K; the horizontal straight line with dots indicates the position of the chemical potential which, to the accuracy of the figure, is the same in all three cases). The lower panel shows the density fluctuation in units of $1/2\pi l_0^2$ for the self-consistent situations (the solid line is for $T = 1$ K and the dash-dotted line for $T = 0.1$ K).

¹ M. A. McCord and D. D. Awschalom, Appl. Phys. Lett. **57**, 2153 (1990).

² H. A. Carmona *et al.*, Phys. Rev. Lett. **74**, 3009 (1995).

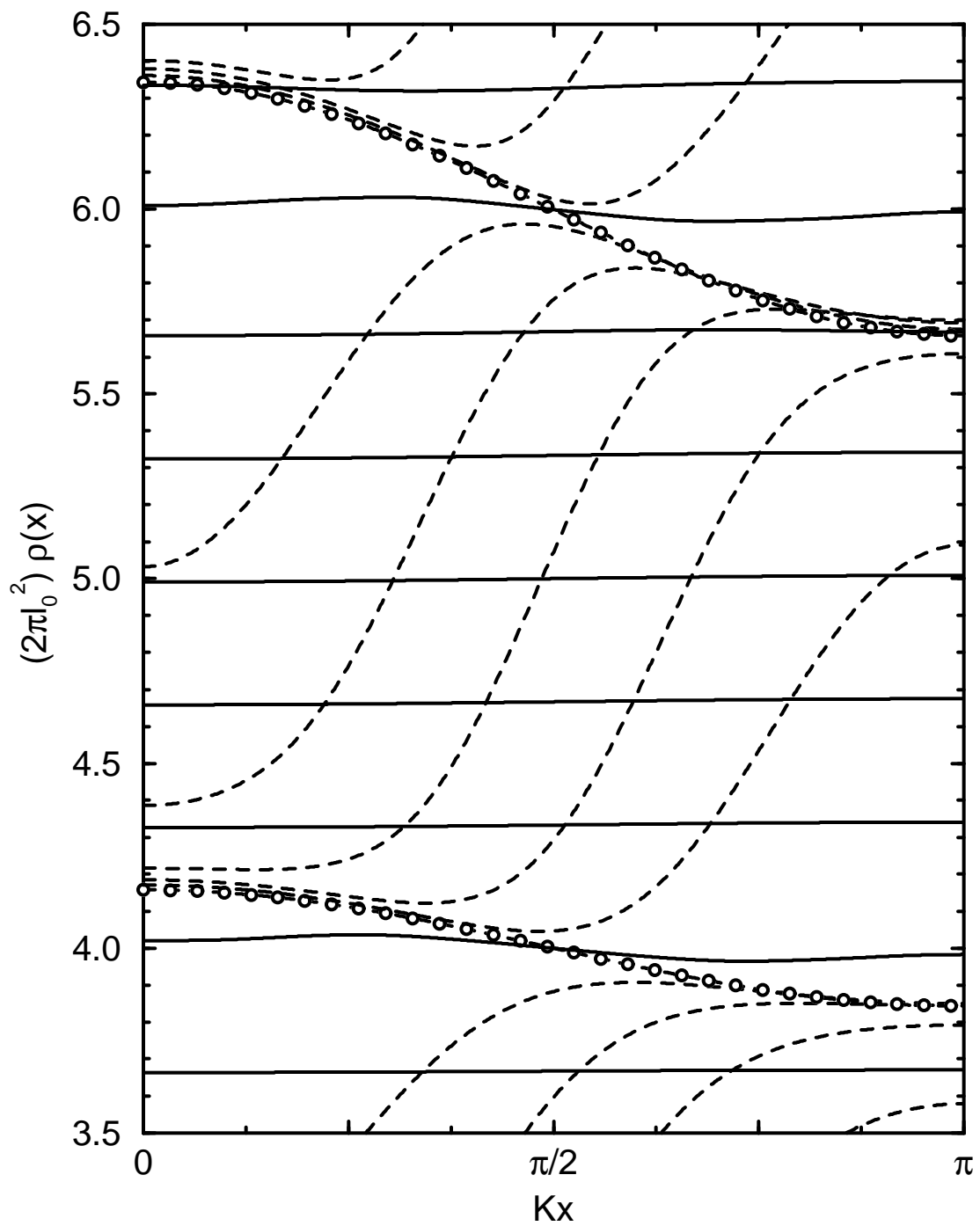
³ P. D. Ye, *et al.*, Phys. Rev. Lett. **74**, 3013 (1995).

FIG. 3. Bandwidth at the Fermi level and amplitude of the induced density fluctuations for the noninteracting systems under a weak magnetic modulation $B_1 = 0.01$ T and an electric modulation $V_1 = 0.27$ meV (leading to comparable maximal bandwidth at the Fermi level, i. e. $v_1 = A_m s$) for average fields $10 \text{ T} > B_0 > 0.125$ T. The data are plotted versus inverse average field indicated on the top x -axis. The bottom x -axis displays the ratio $2R_c/a \propto B_0^{-1}$. (a) shows the width of the band at the Fermi level (solid line for the magnetic, dashed line for the electric modulation; the dash-dotted line is $\hbar\omega_0$). The amplitude of the density fluctuation in units of $1/2\pi l_0^2$ is shown in (b) for the magnetic and in (c) for the electric modulation. The solid lines are for $T = 1$ K and the dashed lines for $T = 0.1$ K and the values for even-integer filling factors are marked with circles or diamonds, respectively. In (c) the dash-dotted line displays the prediction of Thomas-Fermi-theory $|\Delta\rho| = 2(V_1/\mu)\rho_0$.

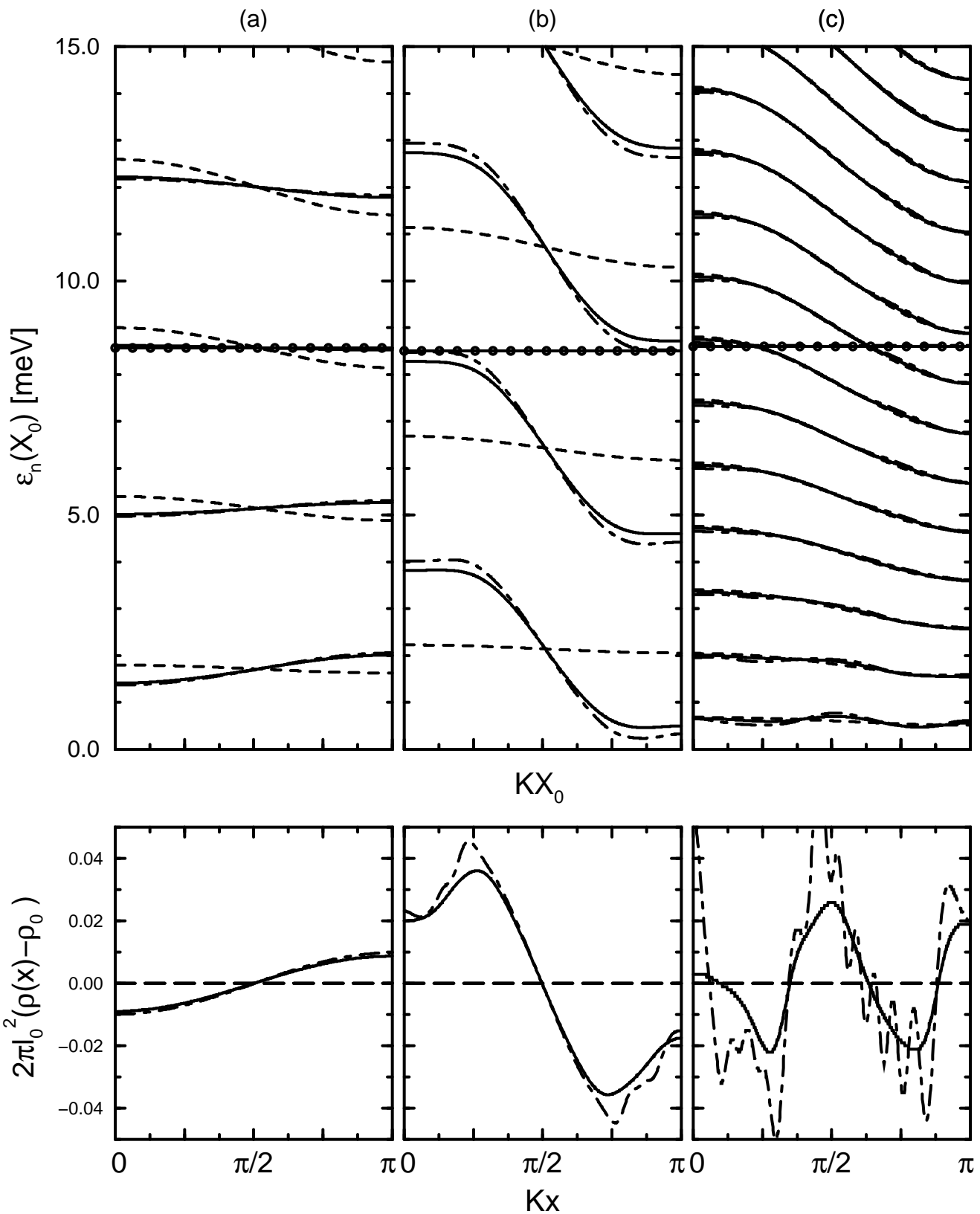
FIG. 4. Bandwidth at the Fermi level and amplitude of density modulation for the noninteracting system as in Fig. 3 but under a stronger magnetic modulation of amplitude $B_1 = 0.1$ T. In (a) the solid line is the width of the band at the Fermi level and the dash-dotted line is $\hbar\omega_0$. (b) displays the amplitude of the density; the solid line is for $T = 1$ K and the dashed line for $T = 0.1$ K; the circles and diamonds mark the values for even-integer filling factors.

FIG. 5. Self-consistent results for a magnetic modulation of amplitude $B_1 = 0.01$ T for $10 \text{ T} > B_0 > 0.18$ T plotted against $2R_c/a$. The upper two panels show for (a) $T = 1$ K and (b) for $T = 0.1$ K the bandwidth $|\Delta\epsilon_{n_F}|$ at the Fermi level (dashed lines with diamonds) and the amplitude of the self-consistent potential $|\Delta V^H|$ (dashed lines with circles). The filling factor was increased in steps of $1/3$ so that each symbol corresponds to a calculated value and the lines are only guides to the eye. The dash-dotted line in (a) and (b) is $\hbar\omega_0$ and the solid line displays the noninteracting bandwidth at the Fermi level for comparison. In (c) the amplitude of the self-consistent densities are shown; here the solid line with circles is for $T = 1$ K and the dashed line with diamonds for $T = 0.1$ K.

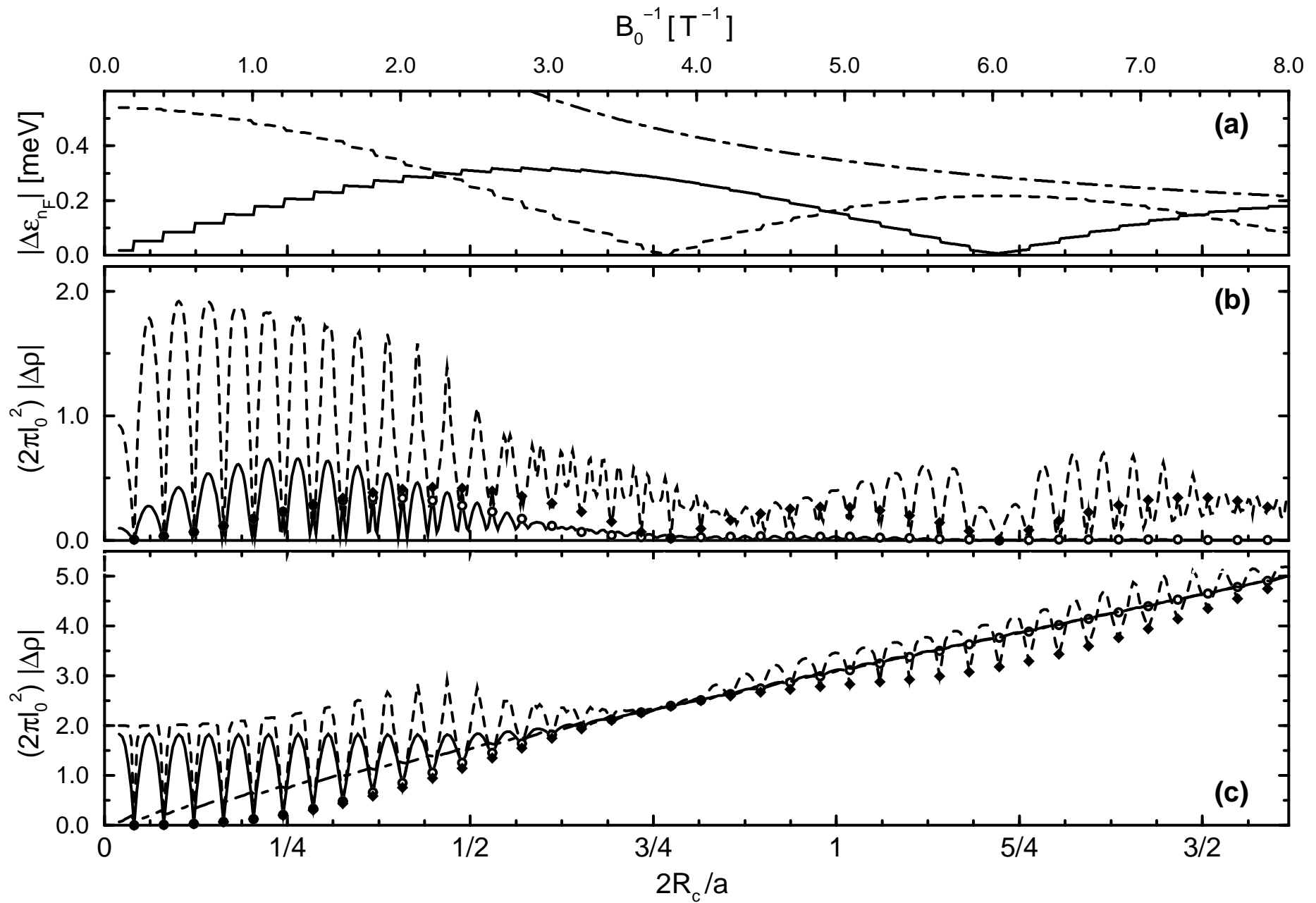
FIG. 6. Self-consistent results for a magnetic modulation of amplitude $B_1 = 0.1$ T and average fields $10 \text{ T} > B_0 > 0.3$ T. The other parameters and the meaning of the lines is the same as in Fig. 5.



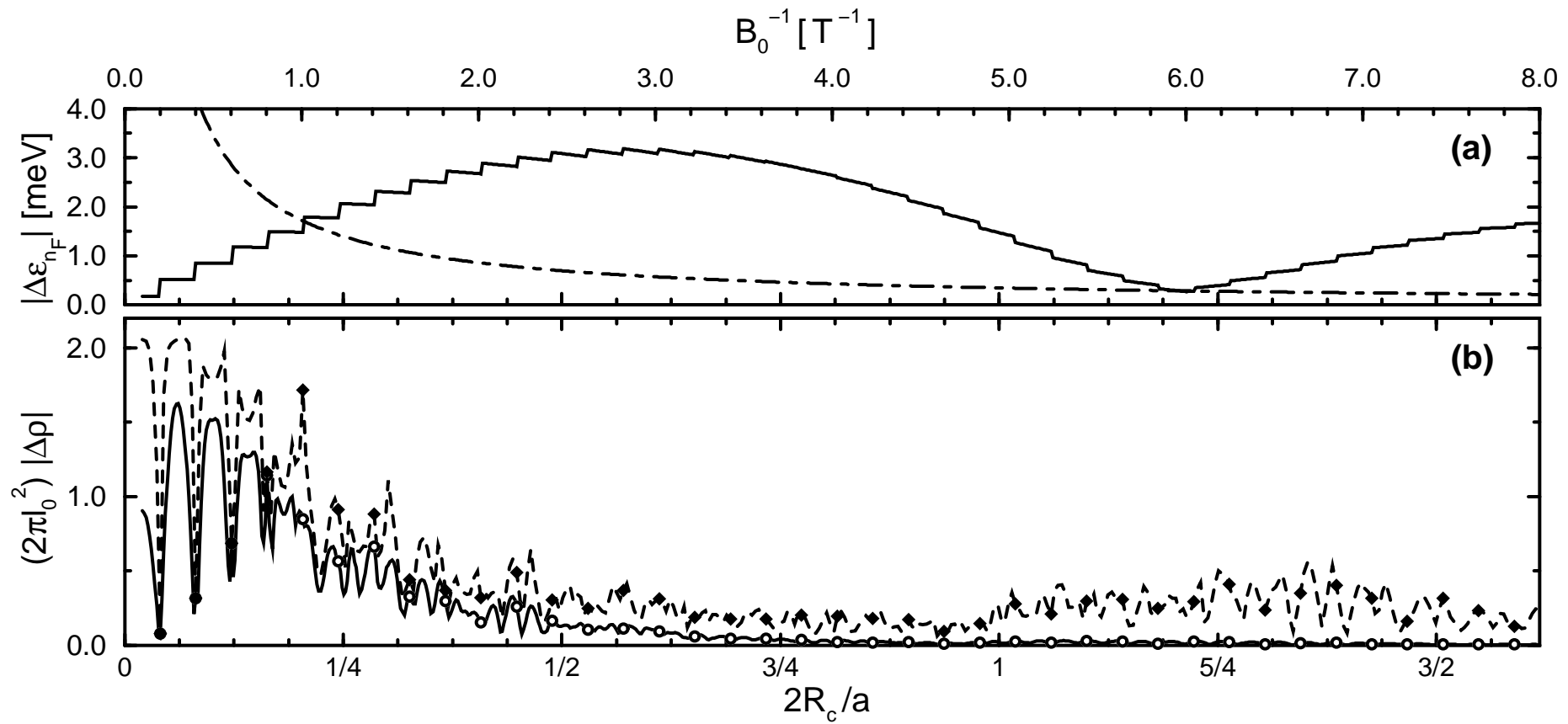
prb gossmann fig 1



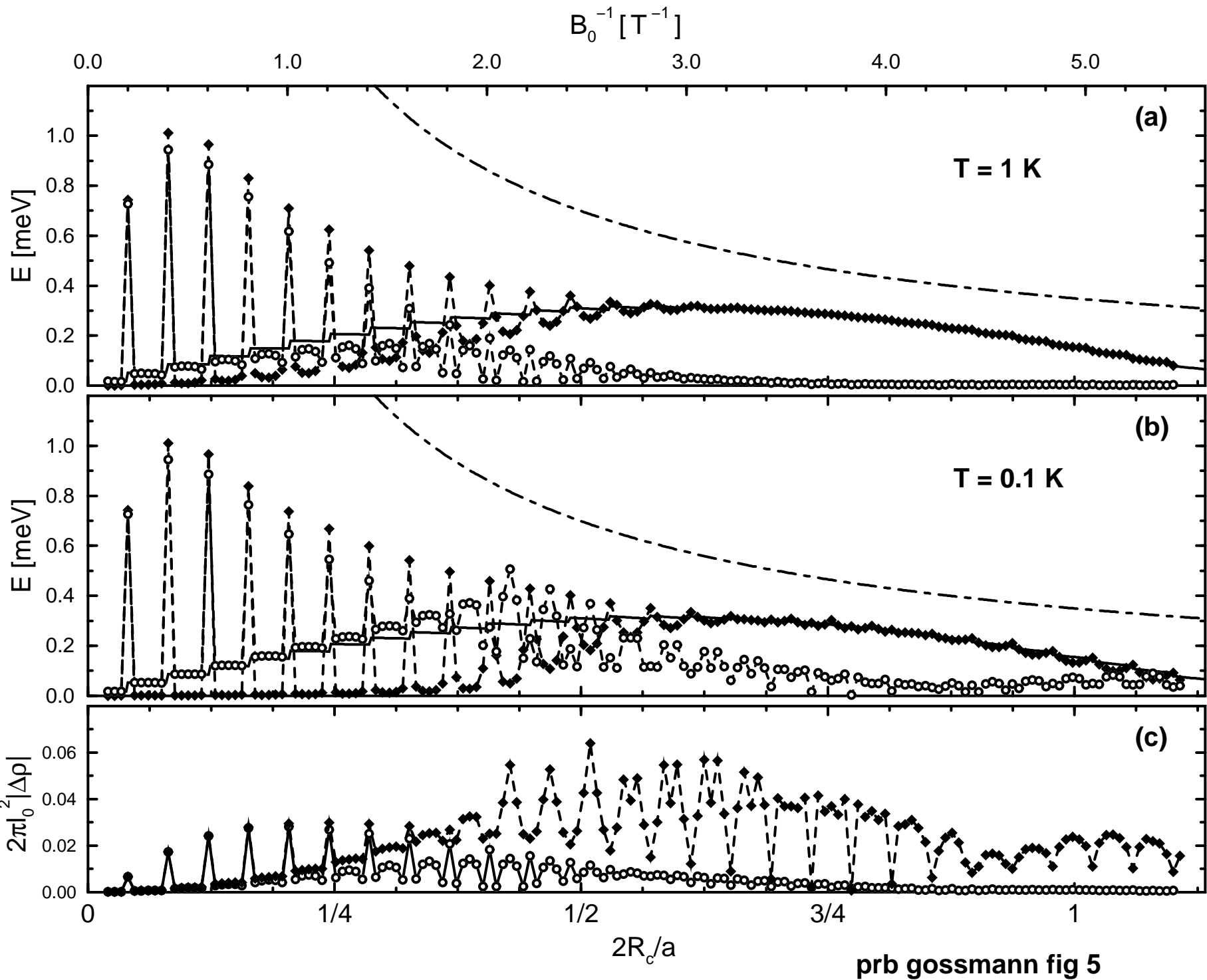
prb goosmann fig 2



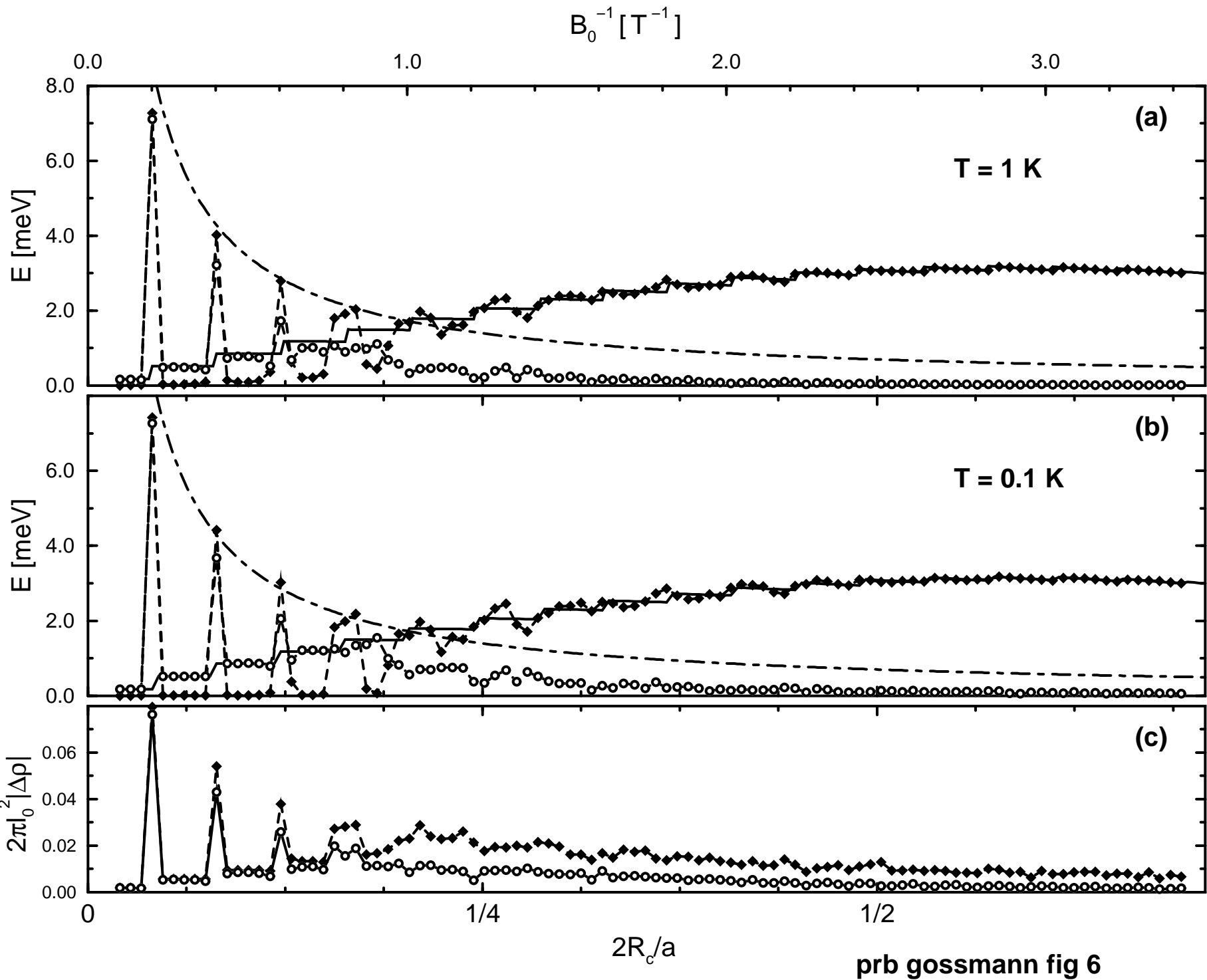
prb gossmann fig 3



prb goosmann fig 4



prb goosmann fig 5



prb goosmann fig 6